Indium segregation in $Gd_5(Si,Ge)_4$ magnetocaloric materials

J. H. Belo,* J. P. Araújo, A. M. L. Lopes, G. N. P. Oliveira, and A. M. Pereira

Institute of Physics of Advanced Materials,

Nanotechnology and Nanophotonics (IFIMUP),

Departamento de Física e Astronomia da Faculdade de Ciências da Universidade do Porto,

Rua do Campo Alegre, 687, 4169-007 Porto, Portugal

Y. Mudryk and D. Paudyal

The Ames Laboratory U.S. Department of Energy,

Iowa State University, Ames, IA, 50011-2416, USA

V. K. Pecharsky

The Ames Laboratory U.S. Department of Energy,

Iowa State University, Ames, IA, 50011-2416, USA and

Department of Materials Science and Engineering,

Iowa State University, Ames, IA, 50011-1096, USA

L. Morellon, P. A. Algarabel, C. Magen, and M. R. Ibarra

Instituto de Nanociencia y Materiales de Aragón (INMA),

CSIC-Universidad de Zaragoza, Zaragoza 50009, Spain and

Departamento de Física de la Materia Condensada,

Universidad de Zaragoza, Zaragoza 50009, Spain

N. Marcano

Centro Universitario de la Defensa,

Academia General Militar Crta. Huesca s/n 50090 Zaragoza, Spain and

Instituto de Nanociencia y Materiales de Aragon,

CSIC-Universidad de Zaragoza, 50009 Zaragoza, Spain

(Dated: September 16, 2021)

Abstract

Chemical substitution is one of the most efficient tools to tune and optimize magnetic and magnetocaloric properties of the giant magnetocaloric materials. In particular, Indium substitutions could be useful both for tuning properties of these interesting intermetallic materials and to unveil their local-scale behavior across the magnetostructural transition via hyperfine techniques. Hence, in order to investigate the effect of Indium additions on the crystal structure, micro-structure, magnetic and magnetocaloric properties, a series of In-containing samples derived from the base $Gd_5Si_{1.2}Ge_{2.8}$ stoichiometry were prepared. The major findings are that while In is insoluble in the 5 : 4 phase, it will instead promote the emergence of the impurity 5 : 3 phase and segregates into this phase. Hence, In leads to major crystallographic changes, which enhance atomic disorder and disrupt the Si to Ge ratio in the 5 : 4 phase. Subsequently, a higher 5 : 4 unit cell volume and a lower magnetic ordering temperature are found in the In-substituted samples. Finally, the magnetocaloric properties of the In-substituted samples reveal a detrimental effect on the maximum magnetic entropy change.

Keywords: Magnetocaloric, rare earth alloys and compounds, phase diagrams, phase transitions, scanning electron microscopy, SEM, magnetic measurements

*Electronic address: jbelo@fc.up.pt

I. INTRODUCTION

Room temperature magnetic refrigeration became more attainable with the discovery of the Giant Magnetocaloric Effect (GMCE) near room temperature (RT) in the $Gd_5Si_2Ge_2$ compound [1]. Particularly in the last decade, intense efforts have been devoted on one hand to the optimization of prototype devices and on the other hand to the understanding of the physical mechanism behind the giant magnetocaloric effect in a wide range of different materials [2–9]. Thus, many $R_5Si_xGe_{4-x}$ compounds (where R is a rare earth element) have been synthesized and studied [4, 10–12], leading to the conclusion that the GMCE is a consequence of a strong coupling between spin and lattice degrees of freedom [13–15]. At RT, an optimal $Gd_5Si_2Ge_2$ sample should crystallize in the monoclinic structure (M) ($P112_1/a$ space group), in the paramagnetic state (PM) [14, 16, 17]. This compound undergoes a simultaneous structural and magnetic (magnetostructural) phase transition to an orthorhombic structure [*O(I)*] (*Pnma* space group) and ferromagnetic (FM) state, [*M*,PM]→[*O(I)*,FM], at its Curie temperature, $T_C \sim 275$ K upon cooling, or when magnetic field or pressure are applied isothermally above T_C [13, 14, 16–18]. In particular, the structural transition occurs from a higher volume monoclinic structure towards a lower volume O(I) structure. These two structures can be seen as a stack of structurally rigid atomic layers along the ac plane which are connected or disconnected to each other if the interlayer Si/Ge3-Si/Ge3 atomic distances are larger or smaller, respectively [19]. The [*M*]→[*O(I)*] structural transition occurs via the adjacent movement of these layers, which leads to the contraction of the interlayer Si/Ge3-Si/Ge3 atomic distances. This magnetostructural phase transition is the physical mechanism responsible for the observed temperature variation of $\triangle T_{ad} \sim 15$ K when a magnetic field of 5 T is applied adiabatically: the so-called giant magnetocaloric effect [1, 13, 14].

Since 1997, a thorough effort has been made to identify and explore different GMCE tuning mechanisms such as application of hydrostatic pressure [15, 20], scale-reduction [9, 21, 22], and chemical substitutions [4, 23–26]. In the later, there are two main possibilities: a) rare-earth (for Gd) substitution and b) transition metal (for Si and/or Ge) substitutions by different chemical elements. In a) the Gd substitutions by Tb and Pr revealed that T_C, and consequently the operational temperature at which the GMCE occurs, decreases with increasing Tb and Pr concentrations, which expectedly, scales with the de Gennes factor

[27]. A similar study was performed on the Gd_5Ge_4 series, where a decrease of the magnetic ordering temperature with increasing concentration of Y was also observed, attributed to the dilution of the magnetic Gd sites by the non magnetic Y atoms [28]. More recently, Rudolph et al. have shown how the Gd substitution by Sc increases T_C up to a critical concentration (where Sc replaces as much as 4 at. % of Gd), while for higher Sc concentrations, a rapid decrease of T_C and a change of the magnetic transition nature (from first to second order) is observed [29]. There are significantly more studies on the Si, Ge substitutions. Generally, it was concluded that the substituting element valence electron concentration (VEC) plays a defining role in the structure stabilization: decreasing VEC (e.g., by substituting Ga for Ge)[30] leads to the stabilization of the O(I) structure, while a VEC increase (e.g., substituting Si by P) leads to the preferential formation of the O(II) structure [31]. Besides changing VEC, there are other factors influencing the structural and magnetic properties of Si, Ge substitutions as illustrated by Pereira and co-workers [32]: by substituting Ge with Fe, the authors have found that the phase composition was significantly altered, in particular by the stabilization of the neighboring 5:3 phase. Such phase was found mostly on grain boundaries and gave rise to long-range strain fields along the 5:4 grains, which mimic the effect of applying hydrostatic pressure.

The presence of the impurity 5:3 phases in $Gd_5Si_xGe_{4-x}$ polycrystalline samples have been detected during the 1960s, when the $R_5Si_xGe_{4-x}$ were originally discovered by Holtzberg et al. [33]. The impurity phases, which tend to appear in addition to the main 5:4 phase with the desired Si:Ge ratio, can be classified in two types: off-stoichiometric (which have the atomic ratio Gd : (Si,Ge) $\neq$ 5:4] [34–37]) and stoichiometric (which have the intended Gd:(Si,Ge) = 5 : 4 ratio, but the Si:Ge ratio is different from the intended stoichiometry [1, 10, 38]). The former phases are, ususally, the closest neighbors of the wanted Gd:(Si,Ge) = 5 : 4 in the Gd-Si-Ge phase diagram (namely the Gd:(Si,Ge) = 5 : 3 and 1 : 1 phases) [39, 40]. In particular, the presence of the neighboring 5:3 is due to a partial eutectoid-like decomposition that occurs during the cooling to RT after solidification [34–36, 39, 40]. On the other hand, the various 5:4 phases form because the x $\sim$ 0.5 composition is just at the border between the M and $M+O(I)$ (phase mixture) regions according to the x-T phase diagram of $Gd_5Si_xGe_{4-x}$ [18, 41]. Thus, the naturally occurring inhomogeneities due to the Si and Ge distribution in the atomic lattice result in different $Si : Ge$ ratios throughout the whole sample volume and consequently in the formation of phases with different atomic and

magnetic structures. A common phenomenon is the formation of phases with Si excess ($x \geq 0.55$), which stabilizes the *O(I)* structure with T_C ranging from 300 K (for $x = 0.55$) to 340 K (for $x = 1$) [14, 41]. The presence of 5:4 and 5:3 phases together in these compounds both decreases the GMCE [14, 42–44], which is critical for technological applications, and complicates the basic study of their rich magnetic properties. Therefore it becomes important to optimize sample synthesis and their corresponding thermal treatments.

In order to broaden the understanding of the atomistic mechanisms controlling the magnetostructural transitions in $Gd_5Si_xGe_{4-x}$ compounds, the hyperfine techniques could be extremely useful since they unveil both the electric field gradients and the magnetic hyperfine fields, potentially revealing each atom$'$s role during the magnetostructural transition. Despite preliminary tests performed with Mössbauer studies [45], there are, to our knowledge, no reports on the Perturbed Angular Correlations (PAC) technique applied to these materials. In most PAC studies, it is required to implant radioactive impurities into the materials lattice, which decay via a double gamma-gamma emission cascade. The angular correlation between the two gamma emissions can be detected and this angular correlation can be perturbed by the interaction of the hyperfine parameters of the host atomic lattice, such as the electric field gradient and the magnetic hyperfine field with the nuclear moments [46–48]. ^{111}In is one of the most commonly used isotopes in PAC studies due to its relatively large half-life and availability.

To our knowledge there has been only one report of minor Indium substitution on Si and Ge sites in the $Gd_5Si_2Ge_2$ compound [49]. Yuzuak et al. have shown that a sample with small Indium content with the nominal $Gd_5Ge_{2.025}Si_{1.925}In_{0.05}$ stoichiometry presents a two-step magnetic transition at $\sim$ 270K and at $\sim$ 298K likely associated with the presence of both M and O(I) atomic structures. Furthermore, the presence of the impurity 5 : 3 phase was detected by x-ray diffraction and the magnetic entropy change was slightly reduced in comparison with the Indium-free parent compound [49]. In order to ensure that the implanted ^{111}In radioactive probe incorporates into the atomic lattice, an important study must be performed before: the assessment of the In substitution location in the material to be studied. In this context, we have performed a thorough evaluation of the effect of In substitutions in $Gd_5Si_xGe_{4-x}$, in particular with $Gd_5Si_{1.2}Ge_{2.8}$ parent composition, on the micro-structural, crystallographic and magnetic properties.

II. EXPERIMENTAL DETAILS

In order to incorporate In in the $Gd_5Si_{1.2}Ge_{2.8}$ compound, three approaches were followed: partially replacing both Si and Ge by In aiming for the following chemical formula - $Gd_5Si_{1.2-0.5x}Ge_{2.8-0.5x}In_x$ (x= 0.05, 0.10 and 0.15); partial replacement of Ge only by In aiming for the $Gd_5Si_{1.2}Ge_{2.8-y}In_y$ (y= 0.10 and 0.30); and, finally, partial replacement of Gd only by In aiming for the $Gd_{5-z}In_zSi_{1.2}Ge_{2.8}$ (z= 0.15 and 0.30). All polycrystalline samples were synthesized by arc melting of the stoichiometric amounts of the constituent elements in purified Ar atmosphere. After the initial melting, three remelts were performed in order to promote homogeneity throughout the samples. Weight losses during the melting were negligible and therefore the as-weighed compositions were assumed unchanged. Additionally, the samples were placed in a quartz tube and were annealed under vacuum (P$<$ 1 x 10^{-5} mbar) at 1473 K for 90 min followed by quenching in water in accordance with previous sample optimization studies [42, 43]. In order to inspect samples morphology and chemical distribution Scanning Electron Microscopy (SEM) combined with Energy Dispersive Spectroscopy (EDS) and x-ray elemental mapping were used. The SEM/EDS setup used in this study was FEI Quanta 400FEG ESEM / EDAX Genesis X4M. SEM and EDS analysis were performed at room-temperature. Room-temperature powder x-ray diffraction (XRD) measurements were performed for all samples (reduced to powders in an agate mortar with an agate pestle) using a Philips X$'$Pert Pro diffractometer with Cu $K_{\alpha 1}$ radiation and in Bragg-Brentano geometry for the $20° \leq 2\theta \leq 90°$ interval. Crystallographic analyses were performed via Rietveld refinements of the XRD patterns using the software package FULLPROF [50]. Superconducting Quantum Interference Device (SQUID) was used to measure magnetization as a function of temperature in the range of 5-300 K and to measure isothermal M(H) curves with applied fields up to μ_0H = 5 T in temperature regions close to the respective magnetic transition temperatures of each sample.

III. EXPERIMENTAL RESULTS

A. Structural Characterization

Powder x-ray diffraction patterns showed that in each sample the main phase crystal structure is O(II). Figure 1 shows details of the XRD patterns of samples where In nominally

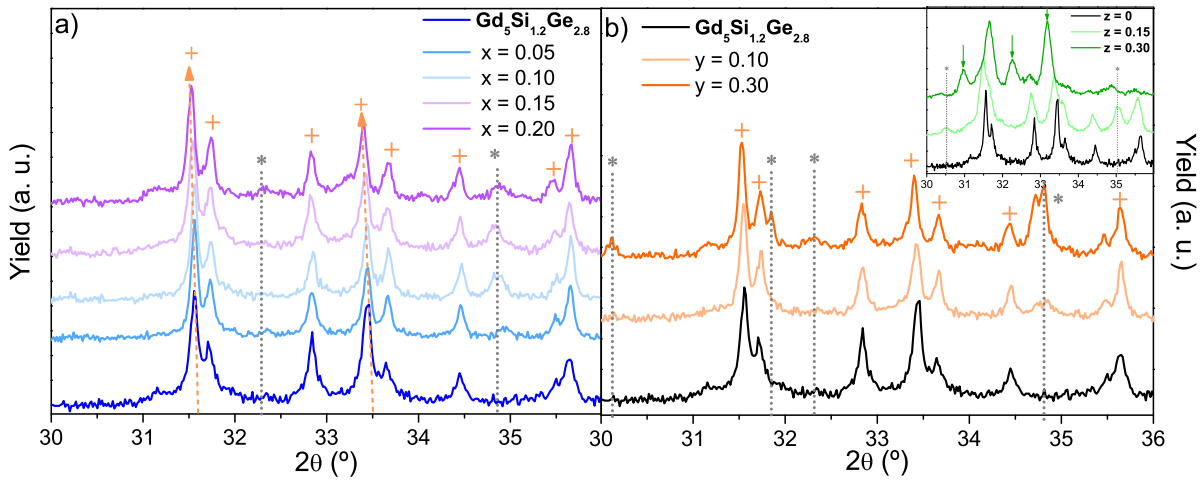

FIG. 1: X-ray diffractograms of Si, Ge (a), only Ge (b), and only Gd (b) inset) In substituted samples in the highlighted 30-36 2θ range, representative of the highest intensity diffracted peaks. The peaks marked as "+" or asterisks represent the Gd:(Si,Ge) $5:4$ and the $5:3$ phases, respectively.

substitutes: Si and Ge (x= $0.05, 0.1, 0.15$ and 0.2) (a)), only Ge (y= 0.1 and 0.3) (b)), and only Gd (z= 0.1 and 0.3) (b) inset) in the 2θ 30°-36° range. In this 2θ interval, which is the region exhibiting the highest intensity Bragg peaks for all samples, there are three main features worth highlighting. The first is the shift of the Bragg peaks of the In substituted samples towards lower angles when compared with the $Gd_5Si_{1.2}Ge_{2.8}$ parent compound, particularly visible in the most intense peaks at $2\theta \sim 31.5°$ and $2\theta \sim 33.4°$, assigned to (1 3 2) and (0 4 2) Miller indices of the Orthorhombic O(II) *Pnma* space group, and marked in Figure 1 with the + signs. For all peaks, the deviation is higher for samples with higher In content, meaning that there is an increase in the O(II) phase unit cell volume. The second main feature is the appearance of new peaks, namely at $2\theta \sim 34.8°$ marked by asterisks in Figure 1 for all In substituted samples (x, y and z $\neq 0$) whose intensity is higher for higher In content samples. This peak is assigned to (1 1 2) of the impurity $Gd_5(Si_xGe_{1-x})_3$ phase, as was also observed in previous studies [43, 51–53]. In addition, extra peaks associated with this phase ($2\theta \sim 32.2°$, $30.2°$ and $\sim 31.8°$) are noticeable in the Ge and Gd substituted samples. In order to extract more information from the XRD patterns and hence confirm the $Gd_5(Si_xGe_{1-x})_3$ phase presence, Rietveld refinement analysis was performed for all samples. For the parent compound, it was sufficient to use the O(II) (*Pnma* space group) phase to fit correctly all peaks in the diffractogram, indicating its single phase nature, whereas for all In

substituted samples (x, y and z $\neq$ 0) the inclusion of the $Gd_5(Si,Ge,In)_3$ ($P6_3/mcm$ space group) phase into the refinement was necessary. The refinement corroborated the $2\theta \sim 34.8°$ peak assignment to the (1 1 2) of the 5 : 3 impurity phase, as initially suggested by peak indexing from literature. The refinements reveal a rapid increase of the concentration of the 5 : 3 impurity phase with the In content, for all In substituted samples as depicted in Figure 2 a). The 5 : 3 phase amount shows an increase up to $\sim$ 8 % for x and z = 0.2, whereas for Ge only substitutions it increases further, up to $\sim$ 12 % for y = 0.3. Interestingly, the weight phase fractions evolve in a similar manner independently of the intended site of the In substitution as can be seen in 2 a). In addition, the O(II) unit cell volume obtained using Rietveld refinement is presented in Figure 2 b) for all In substituted samples. Even though the data are rather scattered, the O(II) unit cell trends higher with increasing In content. The upward trend has one major deviation when y = 0.3.

Interestingly, although the 5 : 4 unit cell volume presents an apparent increase with increasing In amount, not all the unit cell parameters increase, revealing a strong anisotropic behavior. In particular, for the Si,Ge substitutions (x $\neq$ 0), the **a** parameter decreases ($\Delta\mathbf{a}/\mathbf{a} \sim 0.17\%$), whereas **b** ($\Delta\mathbf{b}/\mathbf{b} \sim 0.08\%$) and **c** (($\Delta\mathbf{c}/\mathbf{c} \sim 0.21\%$)) increases with In content. Such anisotropic behavior is similar to the one found along the structural transitions exhibited by these compounds, where the largest changes are observed along the ac plane, in contrast with higher rigidity in b direction. Furthermore, as can be seen in Table S2 of Supplementary Information File, the Si/Ge3-Si/Ge3 interlayer distances exhibit a coherent decreasing tendency regardless of the Indium type substitution, presenting the following relative changes (Δ(Si/Ge3-Si/Ge3)) for each Indium substitution mode: for x = 0.20, Δ(Si/Ge3-Si/Ge3) $\sim$ -9.8%; for y = 0.30, Δ(Si/Ge3-Si/Ge3) $\sim$ -10.0% and for z = 0.15, Δ(Si/Ge3-Si/Ge3) $\sim$ -3.2%. In comparison with the lattice parameters evolution with Indium content in the different substitution types (Table S1), the interlayers Si/Ge3-Si/Ge3 distances present relative variations, which are more than one order of magnitude larger than the lattice parameters variation. In accordance with the relative changes of the unit cell parameters, the interlayers Si/Ge3-Si/Ge3 distances contract mostly along the a-axis.

The O(II) unit cell volume increase may occur due to the In incorporation into the O(II) matrix, which would necessary imply an expansion of the unit cell volume since smaller Si and Ge are being substituted by a larger In atom. However, such reasoning would not explain the increase also observed in the Gd substituted sample, since Gd radius is larger than In,

and therefore a more detailed microstructural characterization is required, discussed in the next section. Moreover the two features observed here, the apparent O(II) unit cell volume increase and the appearance (and increase of concentration) of the 5 : 3 phase amount with increasing content of In with higher atomic radii (than Si or Ge) are common phenomena and have been reported in previous substitution studies, for example for low contents of Sb [54], Sn [55] and Pb [56].

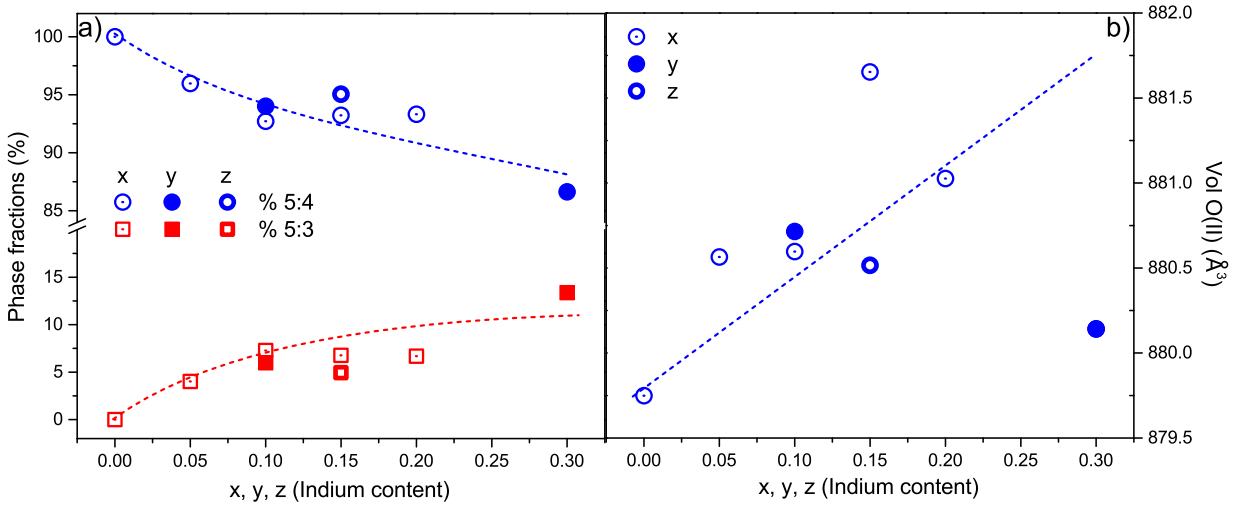

FIG. 2: a) Weight phase fractions of 5:4 (blue circles) and 5:3 (red squares) as a function of Indium content extracted by Rietveld refinements of the x-ray diffractograms for Si,Ge (x substitutions represented as open circles/squares with centered dot), only Ge (y substitutions represented as closed circles/squares) and only Gd-substituted (z substitutions represented as open circles/squares) samples. b) Orthorhombic 5:4 unit-cell volume as a function of Indium content extracted by Rietveld refinements. The dashed blue line is a guide to the eye.

B. Microstructure and elemental mapping

A useful tool to check whether the In atoms are being incorporated into the main O(II) phase or into the impurity 5 : 3 phase is the x-ray elemental mapping, that complements the microstructural and stoichiometric analysis by SEM and EDS. Figure 3 presents the SEM micrograph images obtained by backscattered electrons (in the left column) and the elemental chemical x-ray mapping of the same areas (in the right column) of each of the four elements: Gd, Si, Ge and In. Figure 3 a) is a representative example of the parent

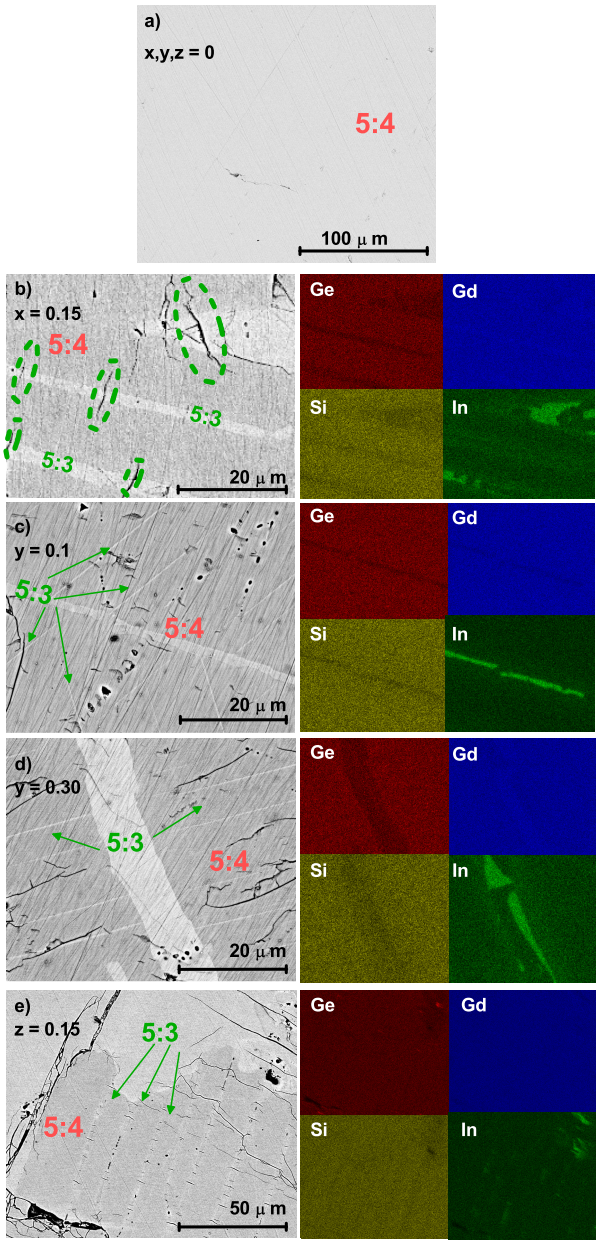

FIG. 3: Scanning electron micrograph produced by backscattered electrons of a) $Gd_5Si_{1.2}Ge_{2.8}$ (x,y,z = 0) parent compound sample, and on the left column of b) $Gd_5Si_{1.125}Ge_{2.725}In_{0.150}$, x = 0.15, c) $Gd_5Si_{1.2}Ge_{2.7}In_{0.1}$, y = 0.10, d) $Gd_5Si_{1.2}Ge_{2.5}In_{0.3}$, y = 0.30, e) $Gd_{4.85}In_{0.15}Si_{1.2}Ge_{2.8}$, z = 0.15. On the right column, the elemental mapping for Gd, In, Si and Ge of the same sample area represented by the micrographs on the left side is shown. In b), c), d) and e) brighter regions are clearly distinguishable from the background darker matrix - such contrast represents phases with different chemical formulae.

compound surface, which reveals a uniform and homogeneous sample where only one phase is detectable, in contrast to what is observed for all samples containing In, Figures 3 b), c), d) and e). EDS was performed in several spots of the observed matrix and the result was a composition close to the nominal $Gd_5Si_{1.2}Ge_{2.8}$ (within a typical 5% error). The micrographs of In-containing samples, where In nominally substitutes for Si and Ge ($x \neq 0$), only for Ge ($y \neq 0$) and only for Gd ($z \neq 0$) are presented in Figures 3 b), c) and d) and e), respectively. A distinctive feature in b)-e) micrographs in comparison with a) is the presence of brighter, typically linear regions within the darker matrix. Because backscattered electron images contrast depends on the average atomic number of the atoms near-surface volume, the brighter regions in these images represent phases with higher atomic number meaning a higher Gd fraction. EDS analysis of these brighter regions shows that their composition is close to Gd:(Si,Ge,In) 5 : 3 phase (within the error bar) with a significantly higher In content than in the darker matrix. This evidence is further supported by the chemical elemental mapping (right column in Figure 3), where in the brighter regions, the Si and Ge maps clearly show darker areas, signalling the low concentration of these elements in the 5 : 3 phase, and Gd maps show brighter areas, signalling the higher content of Gd in these regions. The In mapping also undoubtedly demonstrates that In is rejected from the darker matrix, concentrating within the bright linear features that correspond to the 5 : 3 phase. Interestingly, in the report by Yuzuak and co-workers, a small quantity of the 5 : 3 phase was also observed and EDS analysis unveiled that the majority of the Indium segregated towards this phase [49]. Similar linear and bright features were found previously in the non-substituted $Gd_5Si_xGe_{4-x}$ compounds [35–37, 43, 57, 58] as well as in substituted $Gd_5Si_xGe_{4-x}$ compounds [23, 24, 32, 38, 59] and were also associated with the 5 : 3 impurity phase in the form of In-rich linear strip-like grains. This hypothesis is further corroborated with the x-ray diffractograms where only the In containing samples present peaks which are associated with the 5 : 3 phase. In fact, such contrast is enhanced for samples with higher In content. This observation, together with the x-ray powder diffraction results showing the increase in the 5:3 phase fraction as a function of Indium content presented in Figure 2, represents a strong evidence that Indium segregation promotes the formation and enhancement of linear 5:3 impurity phase regions. Furthermore the x-ray elemental mapping brings more insight about these regions. As can be seen in the elemental maps on the right in Figure 3, these regions are poorer in Si and Ge, retain or slightly increase the Gd amount,

and are richer in In. In the Indium maps the dark/bright contrast is much higher when compared with the other elements, allowing us to infer that only a small amount of In is incorporated into the 5 : 4 darker matrix, whereas the majority of In incorporates in the brighter 5 : 3 phase regions.

On the other hand, both Si and Ge maps show smaller amounts of these elements in these brighter regions, also in accordance with the $Gd_5(Si,Ge,In)_3$ composition hypothesis. Hence, the chemical formulae of these two-phase materials would more appropriately be written as $(1-\alpha)Gd_5(Si,Ge)_4 + (\alpha)Gd_5(Si,Ge,In)_3$. Very similar segregation phenomena occurred also with Fe in Fe-substituted $Gd_5Si_2Ge_2$ samples [32, 38], Ga-substitutions [24] and Co-substitutions [60].

Moreover, Figure 3 b), shows clearly the presence of mechanical cracks transverse to the 5 : 3 strip-like features - highlighted by the dashed green ellipsoids, signaling a stress-strain phenomenon which might be caused by the interplay of the 5 : 3 and 5 : 4 phases and their different mechanical and thermal expansion properties.

C. Magnetic and Magnetocaloric Behavior

In order to characterize the magnetic behavior of all synthesized samples (non-substituted and Indium-substituted x, y and z $\neq 0$), firstly their magnetic susceptibilities as functions of temperature were measured under a magnetic field of 0.05 T. For clarity, only the Si and Ge substituted (x $\neq 0$) magnetic susceptibilities curves are represented in Figure 4 a) (normalized to their maximum value, at T = 5 K). The Ge- and Gd-substituted samples (x = 0, y and z $\neq 0$) susceptibilities are found in Figure S1 in the supplementary information file. The x=0 parent compound sample reveals a sharp paramagnetic to ferromagnetic transition on cooling at T = $T_C \sim 177$ K, in rough accordance with the temperature that should be expected for such composition (168 K) [10]. Such magnetic transition is retained for all x $\neq 0$ samples, however their magnetic susceptibility, $\chi(T)$, curve profiles are significantly changed in the temperature window 100 K< T < 250 K. In particular, slightly above and slightly below T_C, $\chi(T)$ exhibit tail-like features, whose magnitudes are enhanced with increasing In content as can be confirmed in Figure 4 a). The x = 0.05 χ (T) curve exhibits a slightly lower T_C and a broader transition than the parent compound. The x = 0.10 and x = 0.15 χ (T) curves display further T_C decrease and smoothing tendency, in particular for T >

T_C (which will be discussed further below). The T_C evolution with Indium substitution is pictured in Figure 4 b), for Ge/Si substitution ($x \neq 0$), only Ge substitution ($y \neq 0$) and only Gd substitution ($z \neq 0$) as blue open with point in center, red closed and yellow open circles, respectively. These temperatures were assigned as the minima of the temperature derivatives of each magnetic susceptibility curve. Interestingly, for $x \neq 0$ samples, T_C decreases as Indium content (x) increases in a non-linear fashion, which suggests that T_C approaches a constant value for higher In content. In contrast, for $y \neq 0$ and $z \neq 0$ samples, T_C increases with In content in a non-linear fashion too. As will be detailed below, such contrasting T_C behaviors are thought to be a direct consequence of the different Si:Ge ratios within the 5:4 phase, which can lead to a T_C enhancement/reduction and a unit cell volume contraction/expansion if the Si:Ge ratio is larger or smaller than the nominal values [10].

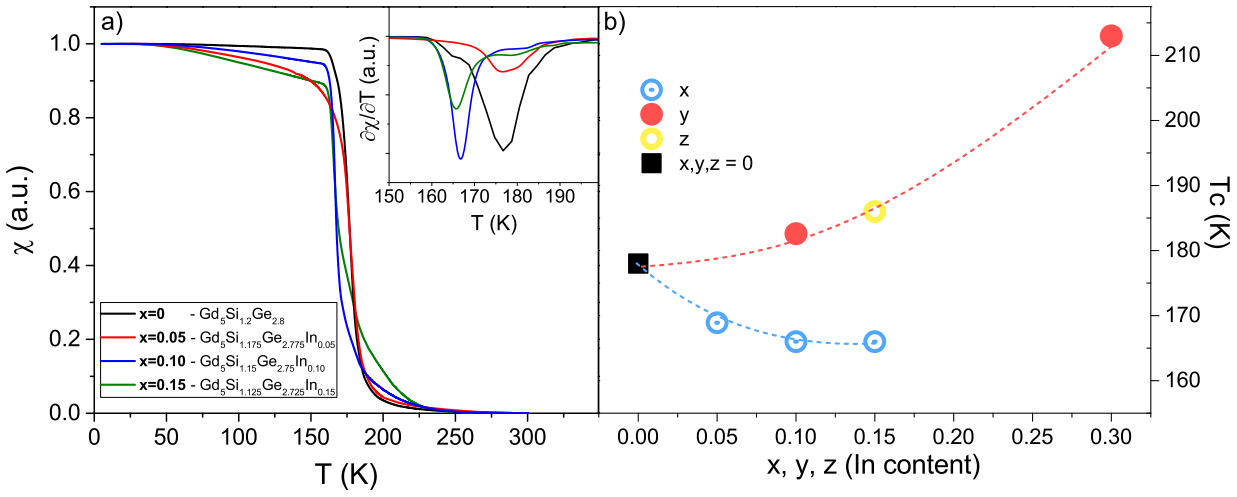

FIG. 4: a) Magnetic susceptibilities as functions of temperature of the parent compound (x=0) and Si and Ge substituted for Indium samples (x=0.05, 0.10, 0.15) normalized to their highest value at T = 5 K. In the inset the temperature derivatives of the magnetic susceptibilities of these samples are presented. b) Curie temperature as a function of Indium content for Ge/Si substitution ($x \neq 0$), only Ge substitution ($y \neq 0$) and only Gd substitution ($z \neq 0$) represented as blue circles, red triangles and yellow squares, respectively.

In order to estimate the saturation magnetization, M vs H isotherms were measured at T = 5 K for all samples (Figure S2 in supplementary information file). The magnetic moments of Gd atom estimated from the saturation magnetization measured at 5 K are listed in Table I.

Apart from sample x = 0.05, which yielded a 15% lower value, all samples exhibited magnetic moments between 7 and 7.7 μ_B in agreement with the theoretical Gd value (7 μ_B per Gd^{+3} ion). Moreover, the reciprocal magnetic susceptibilities as function of temperature (χ^{-1}(T)) were also analyzed for all samples and for x $\neq$ 0 samples they are presented in Figure 5 in the 5 - 300 K range. All χ^{-1}(T) curves exhibit a linear behavior at high temperatures, in the 260-300 K range, in accordance with the expected Curie-Weiss behavior and hence by performing linear fits it was possible to estimate the paramagnetic Curie-Weiss temperatures, θ_p, and the effective magnetic moments, μ_{eff} (values reported in Table I). As can be seen, the θ_p is close to T_C for the x=0 sample, whereas for all the other samples it is consistently smaller than the corresponding $T_C{}'$s for x,y,z $\neq$ 0. As can be seen in Figure 5, for all the x $\neq$ 0 samples $\chi^{-}1$(T) curves exhibit deviations from the linear Curie-Weiss behavior in the $T_C < T < T_G$, where T_G is known to be the Griffiths-like phase formation temperature [61, 62]. In accordance with estimations from previous reports, the parent compound (x=0) has a $T_G \sim 280$ K [4, 62], whereas the x $\neq$ 0 samples exhibit a decreasing tendency for T_G with increasing Indium content, ranging from 280 K (x = 0) to 250 K (x = 0.15).

TABLE I: Magnetic and magnetocaloric properties of Si and Ge substituted $Gd_5Si_{1.2-0.5x}Ge_{2.8-0.5x}In_x$ ($x = 0.05, 0.10$ and 0.15) alloys, alloys with the substitution of Ge by In - $Gd_5Si_{1.2}Ge_{2.8-y}In_y$ ($y = 0.1$ and 0.3) and alloys with the substitution of Gd by In - $Gd_{5-z}In_zSi_{1.2}Ge_{2.8}$ ($z = 0.15$). For the parent compound, x,y,z = 0, T_G value was estimated from [10]. ΔS_m^{MAX} are reported for $\mu_0\Delta H = 5$T.

Chemical formula	x,y,z	Msat	T_C	θ_p	μ_{eff}	T_G	ΔS_m^{MAX}	TEC(15)	TEC(10)
		μ_B	K	K	μ_B/Gd^{+3}	K	J Kg^{-1} K^{-1}	J Kg^{-1} K^{-1}	J Kg^{-1} K^{-1}
$Gd_5Si_{1.2}Ge_{2.8}$	0	-	177	181	8.23	280[10]	46	NA	NA
$Gd_5Si_{1.175}Ge_{2.775}In_{0.05}$	x=0.05	6.00	176	142	7.77	270	43	380	450
$Gd_5Si_{1.15}Ge_{2.75}In_{0.10}$	x=0.10	7.18	164	129	7.38	265	36	270	315
$Gd_5Si_{1.1125}Ge_{2.725}In_{0.15}$	x=0.15	7.4	166	141	7.69	255	26	220	270
$Gd_5Si_{1.2}Ge_{2.7}In_{0.10}$	y=0.10	7.11	183	167	7.32	230	29	260	330
$Gd_5Si_{1.2}Ge_{2.5}In_{0.30}$	y=0.30	7.7	213	176	8.4	250	20	170	210
$Gd_{4.85}Si_{1.2}Ge_{2.8}In_{0.15}$	z=0.15	7.5	186	182	7.1	250	23	210	230

Several M vs H isothermal curves were measured for each sample in order to estimate the

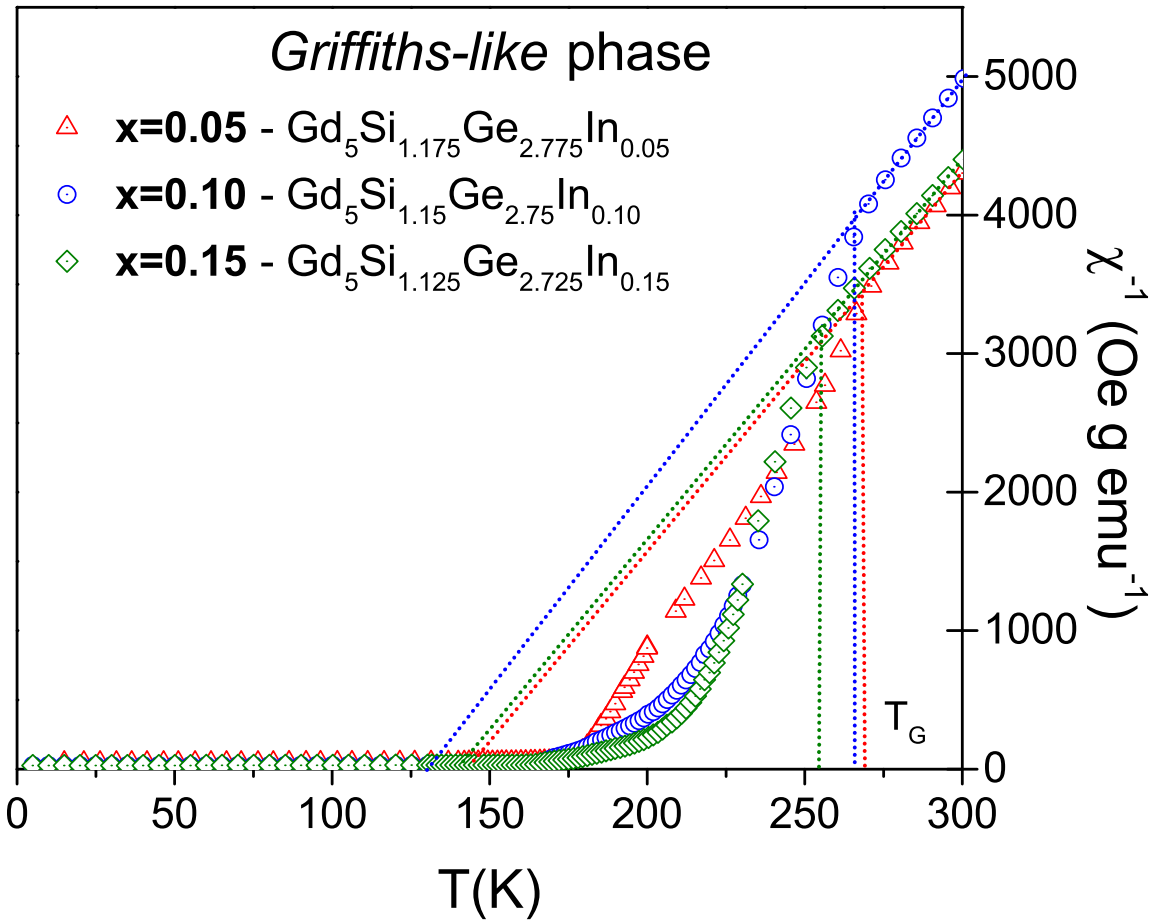

FIG. 5: Inverse magnetic susceptibilities of x $\neq$ 0 samples as a function of temperature plotted together with a linear fit to their highest temperature ranges. The temperature of the deviation from the linear, Curie-Weiss paramagnetic behavior, is highlighted by vertical dashed lines, signalling the onset of the Griffiths-like phase.

magnetic entropy change, ΔSm, for a magnetic field change, $\mu_0\Delta$H = 5 T, as a function of temperature and hence indirectly assess magnetocaloric effect. The ΔSm(T) curves for x,y,z $\neq$ 0 are presented in Figure 6 a). As can be seen, the ΔSm(T) peak value, ΔSm^{MAX}, decreases consistently with the increase of Indium content for all x,y, z $\neq$ 0 samples. In accordance with the T_C versus Indium content evolution there is an increase of the temperature where the peak, ΔSm^{MAX}, is reached for y and z $\neq$ 0 samples. The ΔSm^{MAX} were measured and the temperature averaged entropy change TEC(10) and TEC(15) - a figure of merit to indicate the materials suitability for magnetocaloric cooling applications [63] -

were estimated and their values are reported in the last three columns of Table I.

The Temperature averaged Entropy Change (TEC) is a material-based figure of merit. It is calculated over a range of temperatures, ΔT_{lift}, that a given magnetocaloric material undergoes when is subjected to a specific magnetic field change. It is calculated by dividing the area below a ΔSm curve in a T_{mid} - $\Delta T_{mid}/2$ and T_{mid} + $\Delta T_{mid}/2$, where T_{mid} is chosen by selecting, over the entire ΔSm(T) curve, the temperature value for which TEC(ΔT_{lift}) is maximized [63].

As can be seen, there is an overall decreasing tendency of ΔSm^{MAX}, TEC(10) and TEC(15) values as the Indium content increases, regardless of the In substitution nature. In Figure 6 a), the peak values (ΔSm^{MAX}) are displayed as a function of each sample's respective Curie temperature to the power of -2/3, $T_C{}^{-2/3}$. As can be seen in this figure, regardless of the In substitution, the ΔSm^{MAX} follow a linear trend versus $T_C{}^{-2/3}$, corroborating the expected mean field result discussed in the literature [64, 65].

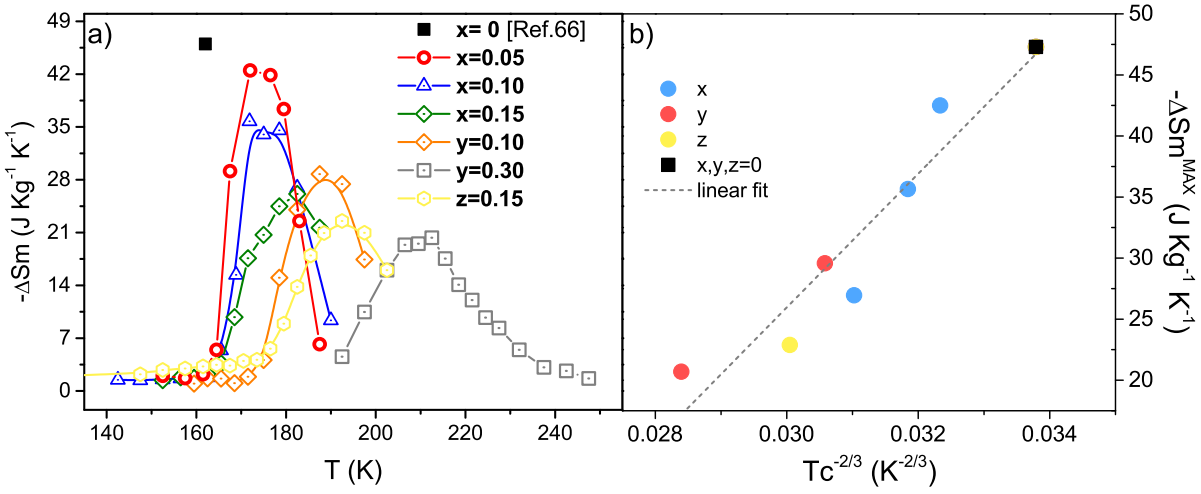

FIG. 6: a) Magnetic entropy change as a function of temperature of parent compound (from reference [66], Si and Ge substituted (x = 0.05, 0.10 and 0.15), only Ge substituted (y=0.10 and 0.30) and Gd substituted (z = 0.15) samples obtained under a magnetic field change of $\Delta\mu_0$H = 5 Tesla. b) Maxima of magnetic entropy change curves are plotted against each respective Curie temperatures to the power of -2/3 together with a linear fit represented by a grey dashed line.

D. Discussion

The extensive characterization of the parent and In-substituted samples presented above calls for a comprehensive discussion in order to analyze the most important features reported here. In particular, from the crystallographic and microscopic characterization it becomes clear that In substitutions lead to the formation of the 5 : 3 phase. As reported in the literature, the 5 : 3 phase is present in the form of In-rich linear strip-like grains with micrometer widths , which are embedded in the majority 5 : 4 phase matrix. In addition to promoting the 5 : 3 phase, elemental x-ray mapping clearly demonstrates that the majority of Indium is not soluble in the 5 : 4 phase matrix, even after high-temperature annealing, but instead, In is almost entirely segregated to the 5 : 3 phase - which explains why the 5 : 3 phase fraction increases with increasing Indium content.

In a previous work [43] it was shown that post-heat treatment similar to the one performed in this work reduces the concentration of the 5 : 3 phase from 25% in as cast sample down to 2-7%. However such behavior was not observed in this work for the In-substituted samples. As follows from the Gd−In phase diagram, Gd_5In_4 phase does not exist, yet the Gd_5In_3 phase forms peritectically in the 35 - 40% Indium atomic concentration range [67]. Hence, despite the care taken with the sample preparation, In-doping promotes the 5 : 3 phase stability at the expense of the 5 : 4 phase.

The formation of the 5 : 3 phase leads to consequences in the microstructure, crystallographic and magnetic properties, namely: i) an enhanced chemical disorder of Si and Ge atoms in both the majority 5 : 4 and the minority 5 : 3 phase, ii) a strain disorder induced by the intermixing of both 5 : 4 and the minority 5 : 3 phase, and iii) the obvious reduction of the overall magnetization change ($\partial M/\partial T$ rate) at the 5 : 4 Curie temperature. The first two consequences lead to the broadening of Bragg peaks and simultaneously to the broadening of the magnetic transition. From previous reports, where the substitutional element was also segregated towards the 5 : 3 phase, the enlargement of the unit cell volume of the 5 : 4 phase has been explained by the Si preferential localization in the 5 : 3 phase [32, 59]. Such Si segregation leads to a Si deficiency in the 5 : 4 phase and, consequently, a higher Ge/Si ratio, which in turn implies a growth of the unit cell volume as reported in the literature [4, 10] and clearly observed in this work for Si,Ge substituted samples ($x \neq 0$). However, interestingly, the Curie temperature behavior as a function of substitutional element content,

i.e. the T_C decrease as In content increases for $x \neq 0$, contrasts with the previous reports where the substitutional element was also segregated towards the 5 : 3 phase and where the T_C increased as a function of substitutional Fe content. Such T_C increase has been explained by the internal strain enhancement induced by the Fe-rich 5 : 3 phase, which would operate similarly to external pressure, reinforcing the magnetostructural coupling and hence enhancing T_C [32]. Although a more detailed study should be performed (namely the comparative study of mechanical properties of the 5 : 4 and 5 : 3 phases), in this work an opposite effect appears to be happening, i.e. a likely Si-deficiency in the 5 : 4 phase leads to the enlargement of the 5 : 4 unit cell. In fact the enlargement of the 5 : 4 unit cell seems to promote cracks transverse to the linear 5 : 3 features as was frequently observed in the SEM micrographs - highlighted by the dashed ellipsoids in Figure 3 b).

As expected by the magnetostructural phase diagram of the $Gd_5(Si,Ge)_4$ family [10], a larger unit-cell volume is associated with weaker magnetic exchange interactions (which can even become antiferromagnetic for large enough unit cells, such as observed in the Gd_5Ge_4 compound) and consequently with lower T_C. Although only one In-substituted sample was studied previously, a T_C reduction in Indium containing sample from $\sim$ 277 K down to $\sim$ 270 K was observed [49].

In contrast to the Si and Ge substituted samples ($x \neq 0$), in the Ge-only substituted samples ($y \neq 0$) T_C increases with the increasing In content. As can be seen in Figure 2 b), the 5 : 4 unit cell volume of $y \neq 0$ does not exhibit a clear tendency (also in contrast with the $x \neq 0$ samples) when In content increases. In this case we believe that there is a trade-off between the Si-deficiency (due to the above mentioned higher Si segregation towards 5 : 3 phase) and the Ge-deficiency (as only Ge is being substituted by In), which is leading to a magnetic exchange interaction enhancement and, consequently, to larger T_C values. Such stoichiometric explanation for the T_C evolution with In content is further supported by the evolution of the Griffiths-like phase ordering temperature, T_G. Although the knowledge about emergence and the nature of the Griffiths-like phase in these compounds is still scarce, there has been consistent evidence that it is intrinsically associated with short-range (few nanometers) magnetically ordered regions whose crystal structure is thought to be low-volume, Gd_5Si_4, O(I) structure [58, 61, 62, 68]. Therefore, T_G should change with Ge/Si ratio in a similar fashion as the T_C of the O(I) structure. Considering such reasoning, it is expected that as the Ge/Si ratio increases, the T_C of the respective O(I) phase decreases

(considering the change in T_G), as, in particular, is clearly observed for the x $\neq$ 0 samples, reported in Table I.

In addition, the tail-like behavior presented by $\chi(T)$ curves below and above T_C, whose magnitude is enhanced with increasing In content (Figure 4 a)), is thought to be associated with the chemical disorder introduced and enhanced by the In content. This is similar to earlier observations in La-substituted $Tb_5Si_2Ge_2$, where despite the complete incorporation of La into the 5 : 4 phase, chemical disorder was also enhanced [23, 68]. In those works we suggested that the partial substitution of La for Tb produced a greater chemical disorder favoring the formation of magnetic clusters in the Griffiths phase and therefore producing an increase in the magnetic susceptibility in the T_C <T <T_G region.

Recently Kou and co-authors [69] found that, despite the different substitution natures, the Zr-substitution on a $Gd_5Si_{1.5}Ge_{2.5}$ sample was shown to induce: similar interlayers Si/Ge3-Si/Ge3 distances contraction as found in this work (Table S2 in Supplementary Information File). In that work the authors argue that interlayers Si/Ge3-Si/Ge3 distances contraction leads to a decrease of Ge population at this atomic position and a decrease of short-range chemical ordering. This hypothesis is sustained by the change in magnetic properties behavior of Zr-substituted samples, which is also observed on our In-substituted samples, namely: 1) the magnetic susceptibility versus temperature curves (χ(T)) exhibit a smoothening near Tc, with the emergence of tail-like features both below and above Tc, leading to a less sharp transition (likely associated with a shift from a 1^{st} order to a 2^{nd} order transition); 2) their T_G also decreases for the substituted samples, and 3) a decrease of the maximum entropy change on substituted samples is observed [69]. The smoothening of the magnetic transition can be explained by emergence of competing magnetic interactions in the substituted samples, via an enhancement of the antiferromagnetic coupling. Whereas the decrease of T_G, can be a direct consequence of the increased chemical disorder.

Finally, the study of the magnetocaloric effect, in particular the ΔSm(T) curves for x,y,z $\neq$ 0 revealed two major changes with In content: the shift of the of the temperature of the ΔSm = ΔSm^{MAX} and the overall decrease of ΔSm^{MAX} regardless of the In-substitution type. A third feature is observed for larger Indium content - the broadening of the ΔSm(T) curve. The latter feature can be understood as a consequence of the enhanced disorder (chemical and strain) with increasing In content - it has been shown that chemical and/or strain disorder leads to broader magnetic transitions, which in turn results in broader ΔSm(T)

curves [70]. The overall decrease of ΔSm^{MAX} and in particular its linear dependence with $T_C{}^{-2/3}$ was also previously theoretically and experimentally shown [64].

IV. CONCLUSIONS

In summary, we found that Indium additions promote the formation of Indium-containing 5 : 3 impurity phase altering the stoichiometries of the main 5 : 4 phase and the materials microstructure. Elemental X-ray mapping clearly demonstrates that Indium is practically insoluble in the 5 : 4 giant magnetocaloric phase regardless of the nominal, as-weighed stoichiometry and is predominantly confined to the 5 : 3 phase. The compositional dependence of the 5 : 4 and 5 : 3 phase fractions with Indium content, as obtained by x-ray diffractograms and their respective Rietveld refinements, corroborate this interpretation as the concentration of the 5 : 3 phase increases with Indium content regardless of the nature of the In substitution. Moreover, the presence and higher content of the 5 : 3 phase has major consequences on the atomic and magnetic structure mostly because it leads to higher atomic disorder and to an unbalance between Si and Ge on the 5 : 4 phase: the 5 : 4 unit cell (O(II)) becomes enlarged and correspondingly the magnetic ordering temperature and the Griffiths-like temperature decreases (this is clearly observable for the Si and Ge substitution). Another consequence of the atomic disorder is the broadening of magnetic susceptibility versus temperature curves, suggesting a change of the magnetic transition nature from first- to second-order and a subsequent reduction of the magnetic entropy change peak with increasing In content. Regardless of the In substitution nature it was observed that the magnetic entropy change peak evolves with $T_C{}^{-2/3}$ as previously derived from the mean-field model. Therefore, with this work it was shown that Indium substitution can tune the atomic and magnetic structure of the giant magnetocaloric material $Gd_5Si_{1.2}Ge_{2.8}$, but in an indirect way as the element segregates in an impurity 5 : 3 phase. In the future, further studies on the miscibility of Indium in 5 : 4 versus in 5 : 3 phase, namely via thermodynamic and kinetic $ab-initio$ calculations could help unveil the Indium role in this system.

Acknowledgments

This work is devoted to the memory of K. A. Gschneidner Jr., an inspiration and guiding light for the magnetocaloric community. Work is partially supported by the projects POCI/CTM/61284/2004, PTDC/CTM-NAN/115125/2009, FEDER/POCTI $n^0155/94$ from Fundacão para a Ciência ex Tecnologia (FCT), Portugal. A.M.P. thanks FCT for the Grant No. SFRH/BPD/63150/2009. J H Belo thanks FCT for the Grant SFRH/BD/88440/2012, the project PTDC/FISMAC/ 31302/2017 and his contract DL57/2016 reference SFRH-BPD-87430/2012. Work at IFIMUP is supported by the following funding projects: POCI-01-0145-FEDER-032527, POCI-01-0145-FEDER-029454 and CERN-FIS-PAR-0005-2017. Work at the INMA is supported by the Spanish Ministerio de Ciencia, Innovacion y Universidades through project $MAT2017-82970-C2$ and Spanish DGA (grant no. $E28-20R$). The research at Ames Laboratory is supported by the Materials Sciences and Engineering Division, Office of Basic Energy Sciences of the U.S. Department of Energy (DOE). Ames Laboratory is operated for the U.S DOE by Iowa State University under Contract No. DE-AC02-07CH11358.

V. REFERENCES

[1] V. K. Pecharsky and K. A. Jr. Gschneidner. Giant Magnetocaloric Effect in $Gd_5Si_2Ge_2$. *Phys. Rev. Lett.*, 78:3–6, 1997.

[2] Andrej Kitanovski, Jaka Tušek, Urban Tomc, Uroš Plaznik, Marko Ožbolt, and Alojz Poredoš. *Magnetocaloric Energy Conversion.* Green Energy and Technology. Springer International Publishing, Cham, 2015.

[3] Gordon J. Miller. Complex rare-earth tetrelides, $RE_5(Si_xGe_{1-x})_4$: New materials for magnetic refrigeration and a superb playground for solid state chemistry. *Chem. Soc. Rev.*, 35:799–813, 2006.

[4] Y. Mudryk, V. K. Pecharsky, and K. A. Gschneidner Jr. *R_5T_4 compounds. An extraordinary versatile model system for the solid state science in: J.-C. Bunzli and V.K. Pecharsky, Eds., Handbook on the Physics and Chemistry of Rare Earths.* Elsevier, v. 44 (2014) pp. 283-449.

[5] V. Franco, J.S. Blázquez, J.J. Ipus, J.Y. Law, L.M. Moreno-Ramírez, and A. Conde. Magnetocaloric effect: From materials research to refrigeration devices. *Progress in Materials Science*, 93:112 – 232, 2018.

[6] A. Rostamnejadi, M. Venkatesan, P. Kameli, H. Salamati, and J.M.D. Coey. Magnetocaloric effect in $La_{0.67}Sr_{0.33}MnO_3$ manganite above room temperature. *Journal of Magnetism and Magnetic Materials*, 323(16):2214 – 2218, 2011.

[7] S. Fujieda, A. Fujita, and K. Fukamichi. Large magnetocaloric effect in $La_5(Fe_xSi_{1-x})_{13}$ itinerant-electron metamagnetic compounds. *Applied Physics Letters*, 81(7):1276–1278, 2002.

[8] D. T. Cam Thanh, E. Brück, N. T. Trung, J. C. P. Klaasse, K. H. J. Buschow, Z. Q. Ou, O. Tegus, and L. Caron. Structure, magnetism, and magnetocaloric properties of $MnFeP_{1-x}Si_x$ compounds. *Journal of Applied Physics*, 103(7):07B318, 2008.

[9] Joao H. Belo, Ana L. Pires, Joao P. Araujo, and Andre M. Pereira. Magnetocaloric materials: From micro- to nanoscale. *Journal of Materials Research*, 34(1):134, 2019.

[10] A.O. Pecharsky, K.A. Gschneidner, V.K. Pecharsky, and C.E. Schindler. The room temperature metastable/stable phase relationships in the pseudo-binary $Gd_5Si_4Gd_5Ge_4$ system. *Journal of Alloys and Compounds*, 338(1):126 – 135, 2002. Special Issue to Honor Professor H. Fritz Franzen.

[11] C. Ritter, L. Morellon, P. A. Algarabel, C. Magen, and M. R. Ibarra. Magnetic and structural phase diagram of $Tb_5(Si_xGe_{1-x})_4$. *Phys. Rev. B*, 65:094405, Feb 2002.

[12] C. Ritter, C. Magen, L. Morellon, P. A. Algarabel, M. R. Ibarra, A. M. Pereira, J. P. Araujo, and J. B. Sousa. Magnetic and crystal structure of $Ho_5(Si_xGe_{1-x})_4$ studied by neutron diffraction. *Phys. Rev. B*, 80:104427, Sep 2009.

[13] L. Morellon, J. Blasco, P. A. Algarabel, and M. R. Ibarra. Nature of the first-order antiferromagnetic-ferromagnetic transition in the Ge-rich magnetocaloric compounds $Gd_5(Si_xGe_{1-x})_4$. *Phys. Rev. B*, 62:1022–1026, Jul 2000.

[14] Vitalij K Pecharsky and Gschneidner Jr. Karl A. $Gd_5(Si_xGe_{1-x})_4$: An Extremum Material. *Adv. Mater.*, 13(9):683–686, 2001.

[15] Cesar Magen, Luis Morellon, Pedro A. Algarabel, M. Ricardo Ibarra, Zdenek Arnold, and Clemens Ritter. Hydrostatic Pressure Effects in the Magnetocaloric Compounds $R_5(Si_xGe_{1-x})_4$. *Advances in Solid State Physics Springer Berlin Heidelberg*, 42:241–253, 2008.

[16] Karl G. Sandeman. Magnetocaloric materials: The search for new systems. *Scripta Materialia*,

67(6):566 – 571, 2012. Viewpoint Set No. 51: Magnetic Materials for Energy.

[17] V.K. Pecharsky, K.A. Gschneidner, Ya. Mudryk, and Durga Paudyal. Making the most of the magnetic and lattice entropy changes. *Journal of Magnetism and Magnetic Materials*, 321(21):3541 – 3547, 2009. Current Perspectives: Magnetocaloric Materials.

[18] A.L. Pires, J.H. Belo, A.M.L. Lopes, I.T. Gomes, L. Morellón, C. Magen, P.A. Algarabel, M.R. Ibarra, A.M. Pereira, and J.P. Araújo. Phase Competitions behind the Giant Magnetic Entropy Variation: $Gd_5Si_2Ge_2$ and $Tb_5Si_2Ge_2$ Case Studies. *Entropy*, 16(7):3813–3831, 2014.

[19] W Choe, V K Pecharsky, A O Pecharsky, K A Gschneidner Jr., V G Young Jr., and G J Miller. Making and Breaking Covalent Bonds across the Magnetic Transition in the Giant Magnetocaloric Material $Gd_5(Si_2Ge_2)$. *Phys. Rev. Lett.*, 84(20):4617–4620, 2000.

[20] L Morellon and Z Arnold and P A Algarabel and C Magen and M R Ibarra and Y Skorokhod. Pressure effects in the giant magnetocaloric compounds $Gd_5(Si_xGe_{1-x})_4$. *Journal of Physics: Condensed Matter*, 16(9):1623–1630, feb 2004.

[21] Ravi L Hadimani, Joao H B Silva, Andre M Pereira, Devo L Schlagel, Thomas A Lograsso, Yang Ren, David C Jiles, and Joao P Araújo. $Gd_5(Si,Ge)_4$ thin film displaying large magnetocaloric and strain effects due to magnetostructural transition. *Appl. Phys. Lett.*, 5(106):32402, 2015.

[22] A. L. Pires, J. H. Belo, J. Turcaud, G. N P Oliveira, J. P. Araújo, A. Berenov, L. F. Cohen, A. M L Lopes, and A. M. Pereira. Influence of short time milling in $R_5(Si,Ge)_4$, R=Gd and Tb, magnetocaloric materials. *Mater. Des.*, 85:32–38, 2015.

[23] J H Belo, A M Pereira, J P Araujo, C de la Cruz, A M dos Santos, J N Goncalves, V S Amaral, L Morellon, P A Algarabel, and M R Ibarra. Tailoring the magnetism of $Tb_5Si_2Ge_2$ compounds by La substitution. *Phys. Rev. B*, 86(1):14403–14412, 2012.

[24] D.M. Raj Kumar, M. Manivel Raja, R. Gopalan, R. Balamuralikrishnan, A.K. Singh, and V. Chandrasekaran. Microstructure and magnetocaloric effect in $Gd_5Si_2(Ge_{1-x}Ga_x)_2$ alloys. *Journal of Alloys and Compounds*, 461(1):14 – 20, 2008.

[25] Y. Mudryk, D. Paudyal, V. K. Pecharsky, K. A. Gschneidner, S. Misra, and G. J. Miller. Controlling magnetism of a complex metallic system using atomic individualism. *Phys. Rev. Lett.*, 105:066401, Aug 2010.

[26] Andrade, Vivian M. and Belo, Joao H. and Reis, Mario S. and Costa, Rui M. and Pereira, André M. and Araújo, Joao P. Lanthanum Dilution Effects on the Giant Magnetocaloric $Gd_5Si_{1.8}Ge_{2.2}$ Compound. *physica status solidi (b)*, 255(10):1800101, 2018.

[27] Y. I. Spichkin, V. K. Pecharsky, and K. A. Gschneidner. Preparation, crystal structure, magnetic and magnetothermal properties of $Gd_xR_{5-x}Si_4$, where R=Pr and Tb, alloys. *Journal of Applied Physics*, 89(3):1738–1745, 2001.

[28] Sumohan Misra and Gordon J. Miller. $Gd_{1-x}Y_xTt_4$ (Tt = Si or Ge): Effect of Metal Substitution on Structure, Bonding, and Magnetism. *Journal of the American Chemical Society*, 130(42):13900–13911, 2008. PMID: 18817384.

[29] Kirk Rudolph, Arjun K. Pathak, Yaroslav Mudryk, and Vitalij K. Pecharsky. Magnetostructural phase transitions and magnetocaloric effect in $(Gd_{5-x}Sc_x)Si_{1.8}Ge_{2.2}$. *Acta Materialia*, 145:369 – 376, 2018.

[30] Hui Wang, Sumohan Misra, Fei Wang, and Gordon J. Miller. Structural and Magnetic Characteristics of $Gd_5Ga_xSi_{4-x}$. *Inorganic Chemistry*, 49(10):4586–4593, 2010.

[31] Volodymyr Svitlyk, Gordon J. Miller, and Yurij Mozharivskyj. $Gd_5Si_{4-x}P_x$: Targeted Structural Changes through Increase in Valence Electron Count. *Journal of the American Chemical Society*, 131(6):2367–2374, 2009. PMID: 19199627.

[32] Pereira,A. M. and dos Santos,A. M. and Magen,C. and Sousa,J. B. and Algarabel,P. A. and Ren,Y. and Ritter,C. and Morellon,L. and Ibarra,M. R. and Araújo,J. P. . Understanding the role played by Fe on the tuning of magnetocaloric effect in $Tb_5Si_2Ge_2$. *Applied Physics Letters*, 98(12):122501, 2011.

[33] F. Holtzberg, R.J. Gambino, and T.R. McGuire. New ferromagnetic 5 : 4 compounds in the rare earth silicon and germanium systems. *Journal of Physics and Chemistry of Solids*, 28(11):2283 – 2289, 1967.

[34] J Szade, G Skorek, and A Winiarski. Surface structure of $Gd_5(Si,Ge)_4$ crystals. *Journal of Crystal Growth*, 205(3):289 – 293, 1999.

[35] O. Ugurlu, L.S. Chumbley, D.L. Schlagel, and T.A. Lograsso. Orientation and formation of atypical Widmanstaetten plates in the $Gd_5(Si_xGe_{1-x})_4$ system. *Acta Materialia*, 54(5):1211 – 1219, 2006.

[36] L.S. Chumbley, O. Ugurlu, R.W. McCallum, K.W. Dennis, Y. Mudryk, K.A. Gschneidner, and V.K. Pecharsky. Linear microstructural features in $R_5(Si,Ge)_4$-type alloys: Difficulties in identification. *Acta Materialia*, 56(3):527 – 536, 2008.

[37] James D. Moore, Kelly Morrison, Garry K. Perkins, Deborah L. Schlagel, Thomas A. Lograsso, Karl A. Gschneidner Jr., Vitalij K. Pecharsky, and Lesley F. Cohen. Metamagnetism Seeded by

Nanostructural Features of Single-Crystalline $Gd_5Si_2Ge_2$. *Advanced Materials*, 21(37):3780–3783, 2009.

[38] Provenzano, V. and Shapiro, A. J. and Shull, R. D. Reduction of hysteresis losses in the magnetic refrigerant $Gd_5Ge_2Si_2$ by the addition of iron. *Nature*, 429:853âĂŞ857, 2004.

[39] Okamoto, H. Gd-Si (Gadolinium-Silicon). *Journal of Phase Equilibria and Diffusion*, 30:213–214, 2009.

[40] Okamoto, H. Gd-Ge (Gadolinium-Germanium). *Journal of Phase Equilibria and Diffusion*, 33:163, 2012.

[41] V.K. Pecharsky, G.D. Samolyuk, V.P. Antropov, A.O. Pecharsky, and K.A. Gschneidner. The effect of varying the crystal structure on the magnetism, electronic structure and thermodynamics in the $Gd_5(Si_xGe_{1-x})_4$ system near x=0.5. *Journal of Solid State Chemistry*, 171(1):57 – 68, 2003.

[42] A. O. Pecharsky, K. A. Gschneidner, and V. K. Pecharsky. The giant magnetocaloric effect of optimally prepared $Gd_5Si_2Ge_2$. *Journal of Applied Physics*, 93(8):4722–4728, 2003.

[43] J.H. Belo and A.M. Pereira and J. Ventura and G.N.P. Oliveira and J.P. Araùjo and P.B. Tavares and L. Fernandes and P.A. Algarabel and C. Magen and L. Morellon and M.R. Ibarra. Phase control studies in $Gd_5Si_2Ge_2$ giant magnetocaloric compound. *Journal of Alloys and Compounds*, 529:89 – 95, 2012.

[44] J. H. Belo, A. M. Pereira, C. Magen, L. Morellon, M. R. Ibarra, P. A. Algarabel, and J. P. Araujo. Critical magnetic behavior of magnetocaloric materials with the Gd_5Si_4-type structure. *Journal of Applied Physics*, 113(13):133909, 2013.

[45] J. C. P. Campoy, A. O. dos Santos, L. P. Cardoso, A. Paesano, M. T. Raposo, and J. D. Fabris. Crystallographic and 119Sn and 155Gd Mössbauer analyses of $Gd_5Ge_2(Si_{1-x}Sn_x)_2$ (x = 0.23 and x = 0.40). pages 191–197, 2009.

[46] Donald R. Hamilton. On directional correlation of successive quanta. *Phys. Rev.*, 58:122–131, Jul 1940.

[47] Edward L. Brady and Martin Deutsch. Angular correlation of successive gamma-ray quanta. ii. *Phys. Rev.*, 74:1541–1542, Nov 1948.

[48] P. Rocha-Rodrigues, S. S. M. Santos, I. P. Miranda, G. N. P. Oliveira, J. G. Correia, L. V. C. Assali, H. M. Petrilli, J. P. Araújo, and A. M. L. Lopes. $Ca_3Mn_2O_7$ structural path unraveled by atomic-scale properties: A combined experimental and ab initio study. *Phys. Rev. B*,

101:064103, Feb 2020.

[49] E Yüzüak and I Dincer and Y Elerman. Giant magnetocaloric effect in the $Gd_5Ge_{2.025}Si_{1.925}In_{0.05}$ compound. *Chinese Physics B*, 19(3):037502, mar 2010.

[50] Juan Rodríguez-Carvajal. Recent advances in magnetic structure determination by neutron powder diffraction. *Physica B: Condensed Matter*, 192(1):55 – 69, 1993.

[51] Vivian M. Andrade, Nathalie B. Barroca, Ana L. Pires, Joao H. Belo, Andre M. Pereira, Kleber R. Pirota, and Joao P. Araujo. Freestanding and flexible composites of magnetocaloric $Gd_5(Si,Ge)_4$ microparticles embedded in thermoplastic poly(methyl methacrylate) matrix. *Materials and Design*, 186:108354, 2020.

[52] Hao Fu, Yungui Chen, Mingjing Tu, and Tiebang Zhang. Phase analysis of $Gd_5(Si_xGe_{1-x})_4$ alloys prepared from different purity Gd with x=0.475 and 0.43. *Acta Materialia*, 53(8):2377 – 2383, 2005.

[53] A.M. Pereira and J.R. Peixoto and D. Leitao and C. Sousa and F. Carpinteiro and P.B. Tavares and N. Martins and J.B. Sousa and J.P. Araújo. Preparation of $Gd_5Si_2Ge_2$ compounds using RF-induction. *Journal of Non-Crystalline Solids*, 354(47):5292 – 5294, 2008. Non-Crystalline Solids 9.

[54] Volodymyr Svitlyk, Yan Yin Janice Cheung, and Yurij Mozharivskyj. Structural, magnetic and magnetocaloric properties of the $Gd_5Si_{4-x}Sb_x$ ($x = 0.5 - 3.5$) phases. *Journal of Magnetism and Magnetic Materials*, 322(17):2558 – 2566, 2010.

[55] J. Q. Li, W. A. Sun, Y. X. Jian, Y. H. Zhuang, W. D. Huang, and J. K. Liang. The giant magnetocaloric effect of $Gd_5Si_{1.95}Ge_{2.05}$ enhanced by Sn doping. *Journal of Applied Physics*, 100(7):073904, 2006.

[56] Y.H. Zhuang, J.Q. Li, W.D. Huang, W.A. Sun, and W.Q. Ao. Giant magnetocaloric effect enhanced by *Pb*-doping in $Gd_5Si_2Ge_2$ compound. *Journal of Alloys and Compounds*, 421(1):49 – 53, 2006.

[57] J.S Meyers, L.S Chumbley, F Laabs, and A.O Pecharsky. Determination of phases in as prepared $Gd_5(Si_xGe_{1-x})_4$, where $x = 1/2$. *Scripta Materialia*, 47(8):509 – 514, 2002.

[58] Ronghui Kou, Zhongwei Chen, Sheng Ouyang, and Jianrong Gao. Phase separation-induced nanoscale heterogeneity in $Gd_5Si_{1.5}Ge_{2.5}$. *Acta Materialia*, 197:163 – 171, 2020.

[59] Bhagya Uthaman, G.R. Raji, Senoy Thomas, K.G. Suresh, and Manoj Raama Varma. Influence of Fe addition on the microstructure, magnetic properties and magnetocaloric behavior of

$Gd_5Si_{1.7}Ge_{2.3}$. *Intermetallics*, 115:106629, 2019.

[60] B. Uthaman, G. R. Raji, S. Thomas, K. G. Suresh, and M. R. Varma. Tuning the Structural Transitions and Magnetocaloric Response in $Gd_5Si_{1.7}Ge_{2.3}$ Alloys Through Cobalt Addition. *IEEE Transactions on Magnetics*, 55(10):1–11, Oct 2019.

[61] C. Magen, P. A. Algarabel, L. Morellon, J. P. Araújo, C. Ritter, M. R. Ibarra, A. M. Pereira, and J. B. Sousa. Observation of a Griffiths-like Phase in the Magnetocaloric Compound $Tb_5Si_2Ge_2$. *Phys. Rev. Lett.*, 96:167201, Apr 2006.

[62] A. M. Pereira, L. Morellon, C. Magen, J. Ventura, P. A. Algarabel, M. R. Ibarra, J. B. Sousa, and J. P. Araújo. Griffiths-like phase of magnetocaloric $R_5(Si_xGe_{1-x})_4$ ($R =$ Gd, Tb, Dy, and Ho). *Phys. Rev. B*, 82:172406, Nov 2010.

[63] L. D. Griffith, Y. Mudryk, J. Slaughter, and V. K. Pecharsky. Material-based figure of merit for caloric materials. *Journal of Applied Physics*, 123(3):034902, 2018.

[64] Belo,J. H. and Amaral,J. S. and Pereira,A. M. and Amaral,V. S. and Araújo,J. P. . On the Curie temperature dependency of the magnetocaloric effect. *Applied Physics Letters*, 100(24):242407, 2012.

[65] H. Oesterreicher and F. T. Parker. Magnetic cooling near Curie temperatures above $300K$. *Journal of Applied Physics*, 55(12):4334–4338, 1984.

[66] K A GschneidnerJr, V K Pecharsky, and A O Tsokol. Recent developments in magnetocaloric materials. *Reports on Progress in Physics*, 68(6):1479–1539, may 2005.

[67] E.M. Mueller Okamoto, M.E. Schlesinger. *ASM Handbook: Gd (Gadolinium) Binary Alloy Phase Diagrams, Alloy Phase Diagrams.* ASM Internation, v. 3 (2016) pp. $379 - 386$.

[68] N. Marcano, P. A. Algarabel, L. Fernández Barquín, J. P. Araujo, A. M. Pereira, J. H. Belo, C. Magén, L. Morellón, and M. R. Ibarra. Cluster-glass dynamics of the Griffiths phase in $Tb_{5-x}La_xSi_2Ge_2$. *Phys. Rev. B*, 99:054419, Feb 2019.

[69] Ronghui Kou, Jianrong Gao, Zhihua Nie, Yandong Wang, Dennis E. Brown, and Yang Ren. Evidence for a short-range chemical order of Ge atoms and its critical role in inducing a giant magnetocaloric effect in $Gd_5Si_{1.5}Ge_{2.5}$. *Journal of Alloys and Compounds*, 808:151751, 2019.

[70] J. S. Amaral and V. S. Amaral. Disorder effects in giant magnetocaloric materials. *physica status solidi (a)*, 211(5):971–974, 2014.

Graphical Abstract: Indium segregation in site substituted $Gd_5(Si,Ge)_4$ magnetocaloric materials

Parent compound:

$Gd_5Si_{1.2}Ge_{2.8}$

- *Indium for **Si,Ge**:* $x \neq 0$, $Gd_5Si_{1.2-0.5x}Ge_{2.8-0.5x}In_x$
- *Indium for **Ge**:* $y \neq 0$, $Gd_5Si_{1.2}Ge_{2.8-y}In_y$
- *Indium for **Gd**:* $z \neq 0$, $Gd_{5-z}Si_{1.2}Ge_{2.8}In_z$

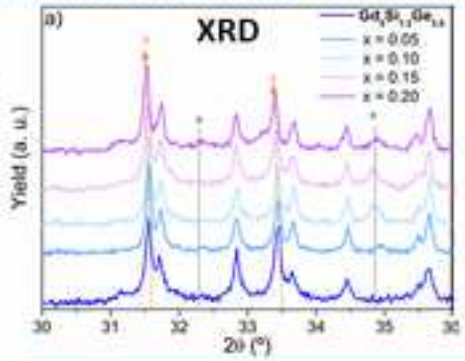

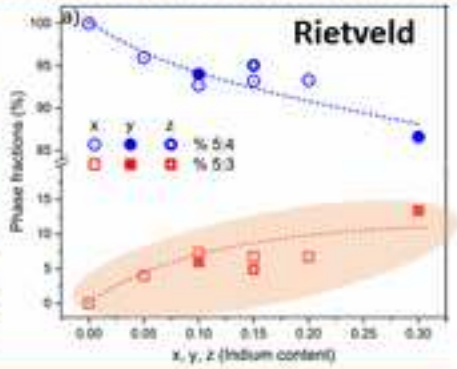

Indium ***promotes*** 5:3 phase fraction

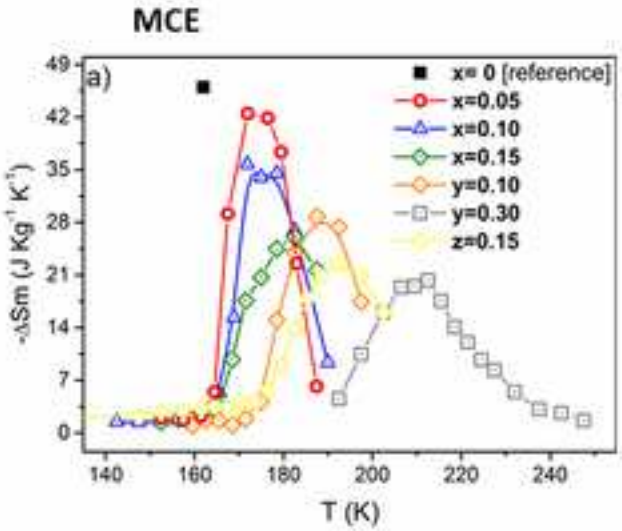

Disruption of Si/Ge ratio in 5:4 phase

increasing disorder

Reduction of ΔSm^{MAX}

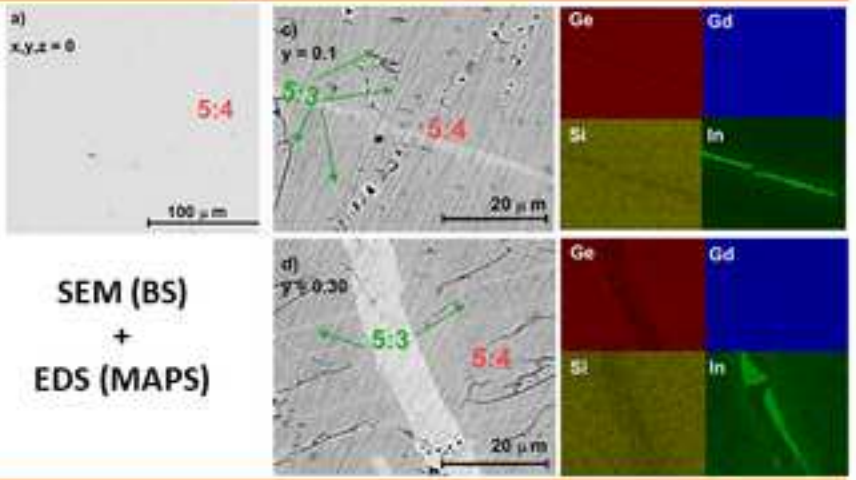

SEM (BS)
+
EDS (MAPS)

Indium ***segregates*** into the 5:3 phase

Highlights

Indium segregation in site substituted Gd5(Si, Ge)4 magnetocaloric materials

João H. Belo[1*], Y. Mudryk[ǂ], D. Paudyal[ǂ], V. K. Pecharsky[ǂ], G. N. P. Oliveira*, A. M. L. Lopes*, L. Morellon[Λ], P. A. Algarabel[Λ], C. Magen[Λ], M. R. Ibarra[Λ], N. Marcano[Ψ], João P. Araújo* and André M. Pereira*

[*] Institute of Physics of Advanced Materials, Nanotechnology and Nanophotonics (IFIMUP), Departamento de Física e Astronomia da Faculdade de Ciências da Universidade do Porto, Rua do Campo Alegre, 687, 4169-007 Porto, Portugal (IFIMUP), Departamento de Física e Astronomia da Faculdade de Ciências da Universidade do Porto, Rua do Campo Alegre, 687, 4169-007 Porto, Portugal;

ǂ The Ames Laboratory U.S. Department of Energy, Iowa State University, Ames, IA, 50011-2416, USA;

ǂ The Ames Laboratory U.S. Department of Energy, Iowa State University, Ames, IA, 50011-2416, USA and Department of Materials Science and Engineering, Iowa State University, Ames, IA, 50011-1096, USA;

Λ Instituto de Nanociencia y Materiales de Aragón (INMA), CSIC-Universidad de Zaragoza, Zaragoza 50009, Spain and Departamento de Física de la Materia Condensada, Universidad de Zaragoza, Zaragoza 50009, Spain;

Ψ Centro Universitario de la Defensa, Academia General Militar Crta. Huesca s/n 50090 Zaragoza, Spain and Instituto de Nanociencia y Materiales de Aragon, CSIC-Universidad de Zaragoza, 50009 Zaragoza, Spain;

E-mail: jbelo@fc.up.pt

- Indium chemical substitution is promising for tuning and for unveiling magnetocaloric atomic scale behaviour:

- Independently of the Indium site substitution on Gd5Si1.2Ge2.8 (by Si and Ge, only Ge and only Gd), Indium is insoluble in the magnetocaloric 5:4 phase.

- Instead, Indium promotes the impurity 5:3 phase and segregates almost completely in this 5:3 phase;

- Indium substitution promotes: atomic disorder, disruption of Si/Ge ratio on the 5:4 phase, increase of unit cell volume and has a detrimental effect on Gd5Si1.2Ge2.8 magnetocaloric effect.

Figure 3

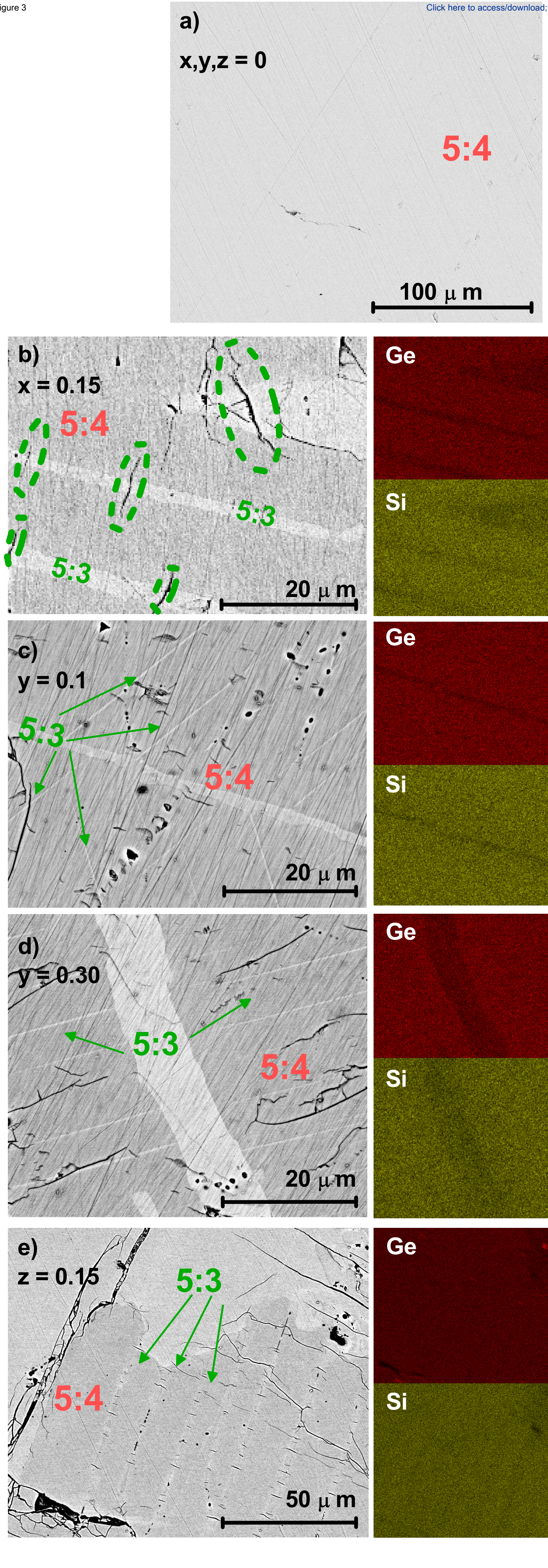

Figure 4

Click here to access/download;Figure;Figure4_MTs_new2_rere-eps-converted-to.pdf

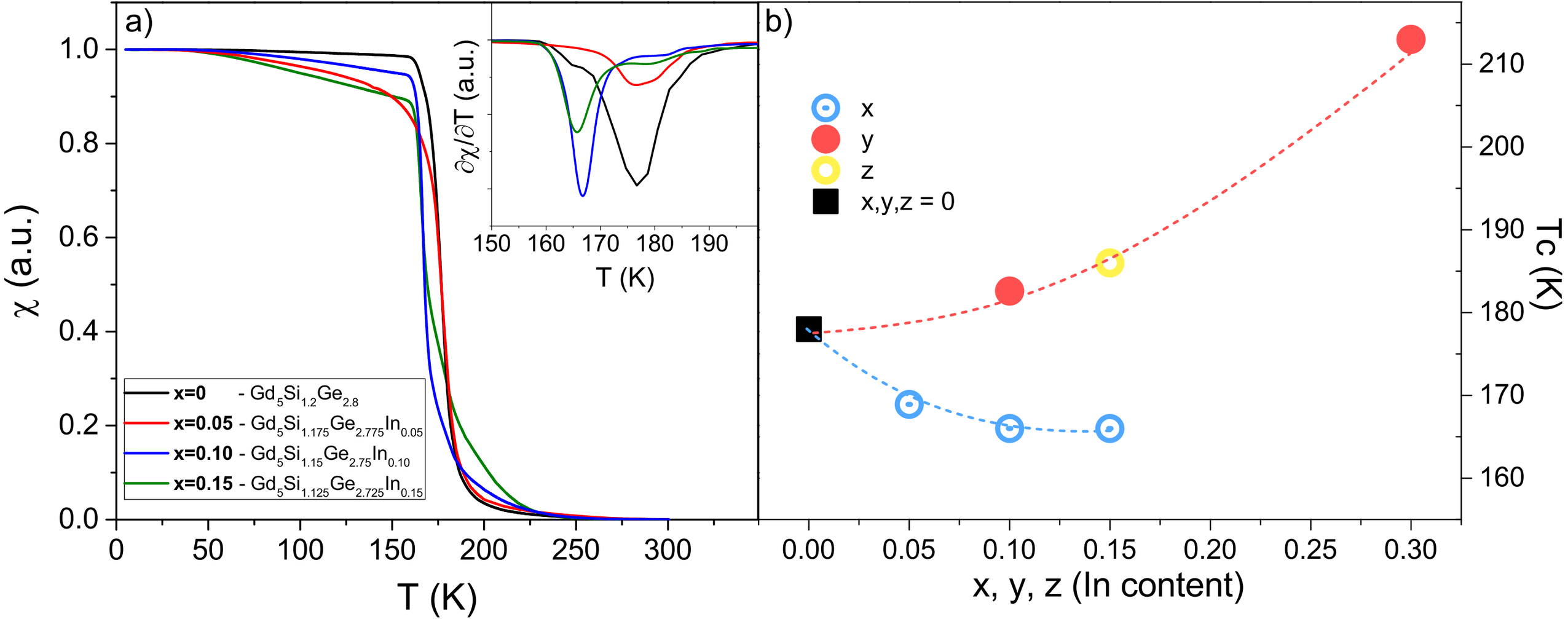

Figure 5

Click here to access/download;Figure;Figure5_InvSusc_new-eps-

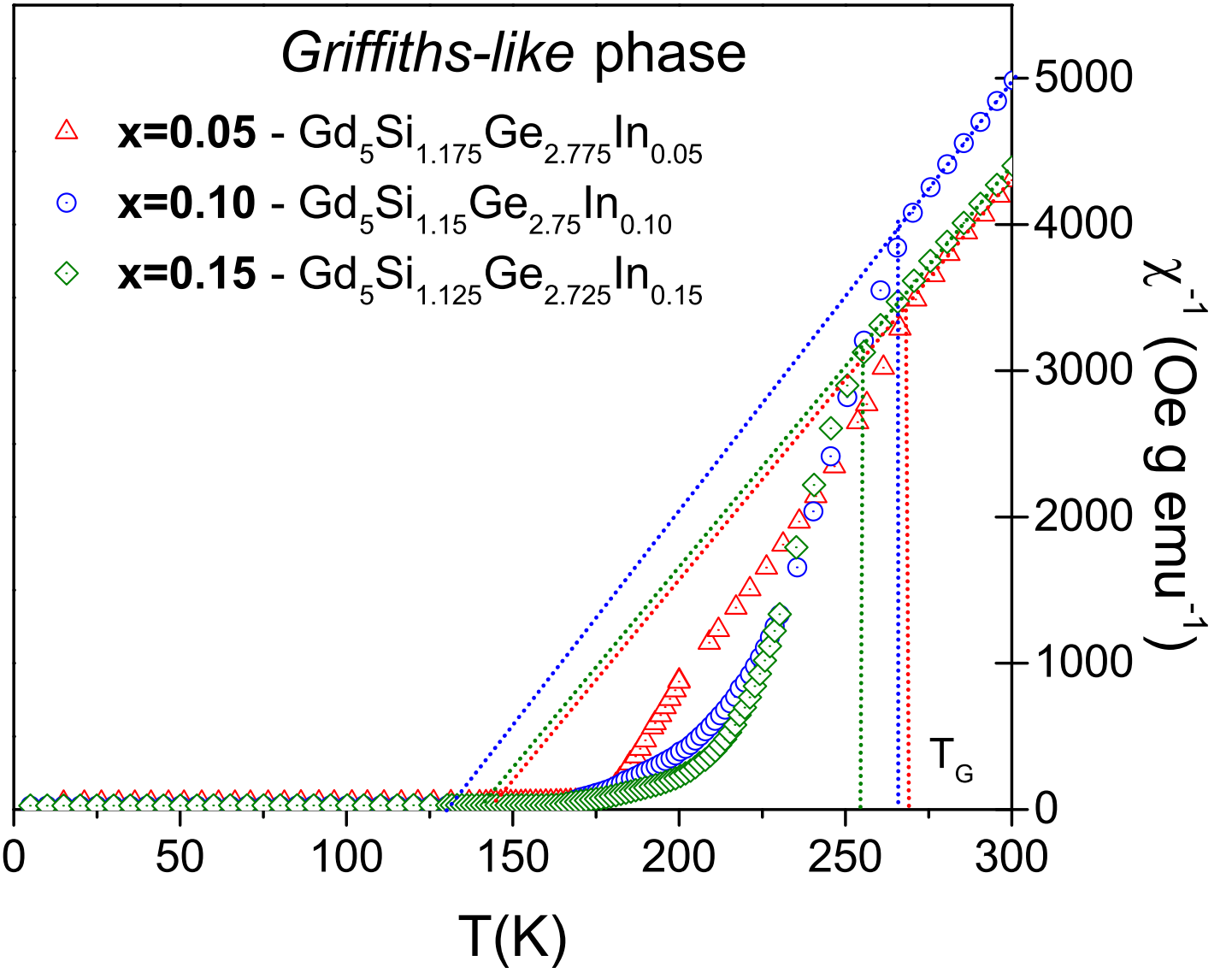

Figure 6

Click here to access/download;Figure;Figure6_MCE_new_re-eps-converted-to.pdf

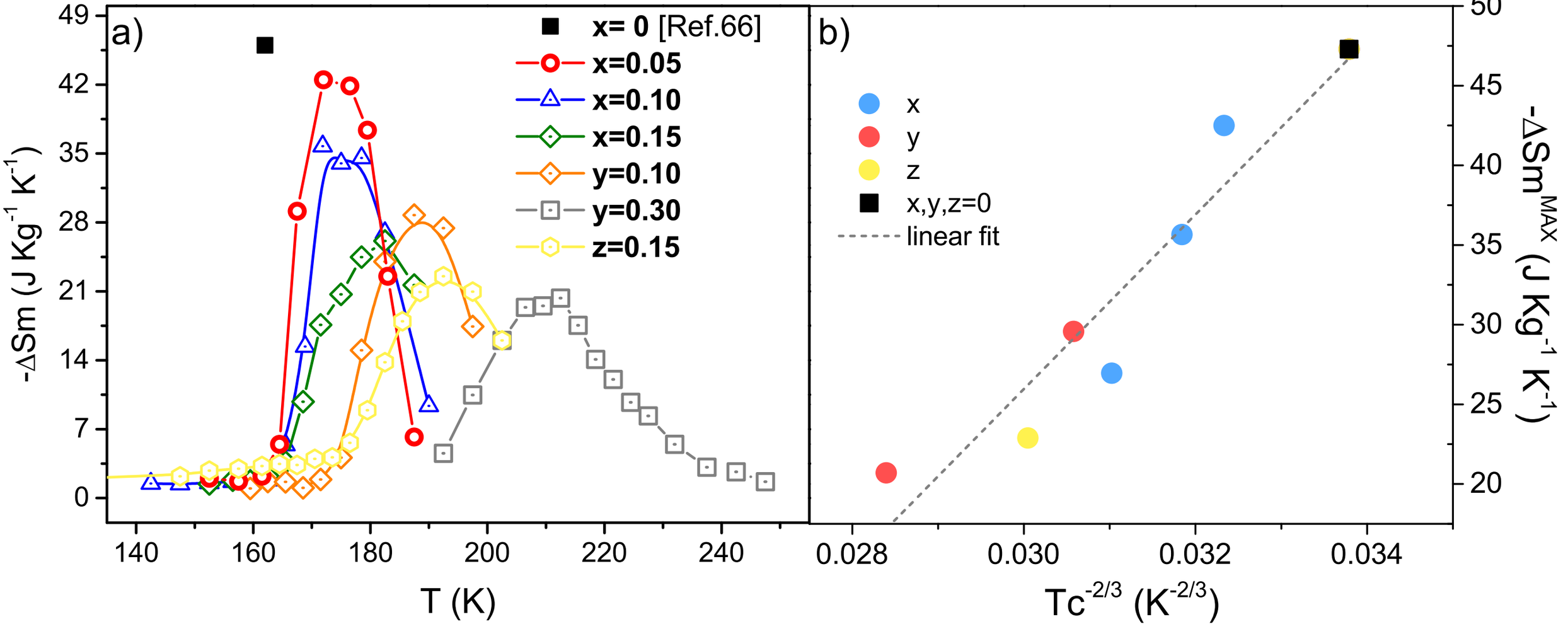

Figure 1

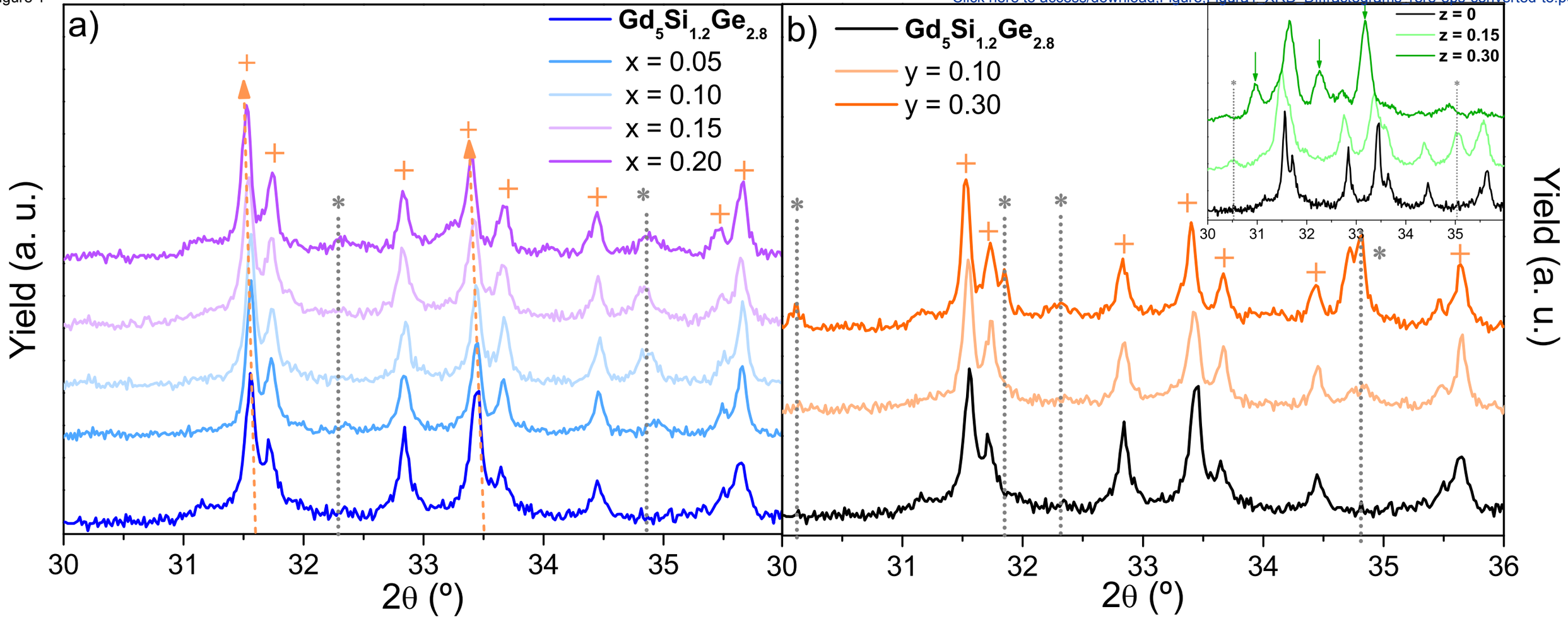

Figure 2